Land–biosphere–atmosphere interactions over the Tibetan plateau from MODIS observations

2012 Environ. Res. Lett. 7 014003

(http://iopscience.iop.org/1748-9326/7/1/014003)

IOP PUBLISHING ENVIRONMENTAL RESEARCH LETTERS
Environ. Res. Lett. **7** (2012) 014003 (9pp) doi:10.1088/1748-9326/7/1/014003

Land–biosphere–atmosphere interactions over the Tibetan plateau from MODIS observations

Menglin S Jin and Terrence J Mullens

Department of Meteorology and Climate Science, San Jośe State University, CA 95119, USA

E-mail: jin@met.sjsu.edu

Received 5 October 2011
Accepted for publication 9 December 2011
Published 4 January 2012
Online at stacks.iop.org/ERL/7/014003

Abstract
Eleven years (2000–10) of monthly observations from the National Aeronautics and Space Administration (NASA) Terra Moderate-resolution Imaging Spectroradiometer (MODIS) show the diurnal, seasonal, and inter-annual variations of skin temperature over the Tibetan plateau (75–100°E, 27–45°N) at 0.05° × 0.05° resolution. A slight warming trend is observed during this period of time, although the relatively short duration of the observation makes such a trend uncertain. More importantly, using the most recent climatology of land skin temperature, spatially high correlation coefficients are found among normalized difference vegetation index (NDVI), water vapor and cloud relations, indicating that the land surface, vegetation and atmosphere influence one another. Such a quantitative understanding of these relationships at high spatial resolution would be helpful for modeling the biosphere–atmosphere–land surface interaction processes over the Tibetan plateau.

Keywords: Tibetan plateau, land surface–biosphere–atmosphere interaction, surface warming, remote sensing

1. Introduction

Monitoring the land surface, biosphere and atmosphere conditions of the Tibetan plateau has always been a challenge because of the high elevation of the region. Satellite remote sensing provides high spatial and high temporal resolution observations and thus is extremely useful for study over the Tibetan plateau. This letter examines the 2000–10 land surface skin temperature from the diurnal, seasonal and inter-annual perspectives, using satellite observations from the National Aeronautics and Space Administration (NASA) Terra and Aqua Moderate-resolution Imaging Spectroradiometer (MODIS). An unique advantage of MODIS data is that it provides consistent measurements for the land surface, the biosphere and the atmosphere simultaneously including, skin temperature, land cover, normalized difference vegetation index (NDVI), snow cover, cloud, water vapor and other variables (Jin and Dickinson 2010). Jointly analyzing these variables will clarify which land surface–biosphere–atmosphere interactions are responsible for skin temperature variations.

Decadal MODIS observations show that the surface skin temperature over Tibetan plateau during 2000–10 varies spatially, depending on land cover, vegetation and elevation. Over the whole region, skin temperature has shown a slight increasing trend during 2000–10. A significant warming trend is obtained at nighttime. In addition, vegetation, water vapor and clouds are closely related to skin temperatures and the underlying evapotranspiration. Our results provide independent, additional support for previous climate change studies over that region, and new insights on biosphere–land temperature interaction, which may partly explain surface warming over that region.

Previous studies have emphasized identifying surface temperature trends in the Tibetan region and the impacts of such trends, if any. Liu and Chen (2000) reported a warming in the Tibetan region as a whole as well as on most of the

ground sites. Wang *et al* (2008) outlined warming in the past 60 years from surface 2 m observations and then, using a model, suggested that the warming of the Tibetan plateau may lead to a precipitation enhancement in East Asia. Warming the Tibetan plateau leads to instability of the atmosphere, resulting in local convective precipitation. This increase in latent heat strengthens the South Asian high pressure system at the upper levels promoting an increase in rainfall in East Asia.

These previous studies on surface temperature change used the 2 m shelter temperature measurements, which are located at only a few sites over the plateau leaving large areas with no observations. Greater areal coverage with fine resolution observations, such as those from satellite remote sensing, will contribute to a better understanding of the regional climate of the Tibetan plateau. This is the motivation of this letter.

In addition to identifying surface temperature variations, understanding the physical mechanisms responsible for the variations is equally important. Land–biosphere interactions affect the skin temperature. Increases in the 2 m surface temperatures, NDVI and precipitation (Chu *et al* 2007) have been reported. NDVI, an index of the greenness and growth of vegetation (Tucker *et al* 1986), shows that a change in vegetation leads to local and regional climate variations (Chu *et al* 2007). This perspective is further examined here using new MODIS high resolution measurements.

Atmosphere conditions also affect surface temperature. Water vapor in the Tibetan plateau has a clear seasonality with winter being the driest and summer the wettest (Jin 2006) directly affecting the formation of cirrus clouds (Gao *et al* 2003). Furthermore, due to the high altitude and low surface temperature, water vapor over the plateau is less than the global average (Jin 2006). Nevertheless, the southeast portion of the plateau is slightly moister than the rest of the plateau due to southeast monsoonal flows (Wu and Zhang 1998) and abundant vegetation evaporation, a fact that affects skin temperatures in the area. In addition, a significant increase in the amount of low-level clouds has been reported (Duan and Wu 2006), which may explain, at least partly, the surface air temperature increase at nighttime due to the 'greenhouse effect' of clouds.

Tibet features a semi-arid continental climate, and the surface temperature largely depends on the orographic effects of the Himalayan Mountains to the south. Coinciding with the Asian monsoon, most precipitation occurs between May and September (Yeh *et al* 1957, Wu and Zhang 1998, Wu *et al* 2004) with the southeastern region of the plateau receiving the most precipitation and the northwestern region the least. The pattern of precipitation has been attributed to the southeasterly flow of the monsoon and the low-lying terrain in the southeast region (Wu and Zhang 1998). This letter supports this hypothesis by showing high water vapor content in the southeast part of the Tibetan plateau where high vegetation cover lead to relatively high evapotranspiration.

Section 2 briefly discusses the satellite data sets used in this analysis, followed by results analysis (section 3). Section 4 discusses the uncertainty of this study as final remarks.

2. Data

MODIS skin temperature observations (Wan and Li 2008) during 2000–10 are used to examine whether the Tibetan plateau has warming according to this radiometric temperature field. Skin temperatures are measured by the MODIS instrument on NASA's Terra satellite, launched in December 1999, and NASA's Aqua satellite, launched in May 2002. They are measured using seven thermal infrared bands at 10:30 local time (LT) and 22:30 LT daily (Terra) and 13:30 LT and 1:30 LT (Aqua), i.e., four times per day. Each pixel has a 1 km resolution at nadir, which has been scaled up to a $0.05° \times 0.05°$ resolution as well as averaged to monthly values as a MODIS standard product. Only values with quality flags indicating the absence of clouds are used.

The NDVI data, which represents vegetation greenness (Myneni *et al* 1995) and was derived from 16-day data for the 11 yr period between 2000 and 2010, is correlated with skin temperature. The NDVI product is derived from bands 1 and 2 of the MODIS Terra satellite. A time-series of NDVI observations can be used to examine the dynamics of the growing season or how it is related to skin temperature changes.

MODIS snow cover (Hall *et al* 2002, Hall and Riggs 2007) is analyzed to understand the reasons for low skin temperature in winter and the effects. An index with values from 0 to 100 indicates whether are region is snow free or 100% snow-covered. Pixels that either contain clouds or undetectable with snow, are given values beyond 100 and treated as missing data in our analysis.

The most recent version of MODIS atmosphere products (so-called collection 5) are analyzed for the same period of time (2000–10) (King *et al* 2003, Gao *et al* 2003). In particular, the cloud fraction and total column water vapor from Terra MODIS observations during the daytime (10:30 AM) are used here to examine whether cold surfaces are related to water vapor and cloud cover. All the MODIS observations that are analyzed are collection five data at spatial resolutions of $0.05° \times 0.05°$ for land cover, snow cover, NDVI, and $1° \times 1°$ for the atmosphere variables.

There are three sources of uncertainty in satellite derived skin temperatures. The first is cloud contamination. MODIS uses thermal infrared bands to monitor surface temperature and will never be able to measure skin temperature under cloudy skies. Therefore the MODIS skin temperature measurements analyzed in this letter are only for clear skies. This creates an uncertainty in the warming trend indicated in this letter. How cloud amount changes and skin temperature changes for a full-sky condition (clear and cloudy days) remain unknown. Therefore, a cloud adjustment scheme (as discussed in Jin 2000, Jin and Dickinson 2000) might be a practical way to solve such a problem. Second, the emissivity, a parameter needed in skin temperature retrieval, is unknown for the heterogeneous surface of the Tibetan plateau. Third, due to the high land surface heterogeneity, each pixel of the satellite generally contains more than one land type, but MODIS only calculates one skin temperature value for this pixel. It is challenging to interpret this one skin temperature, given the different sub-pixel land types.

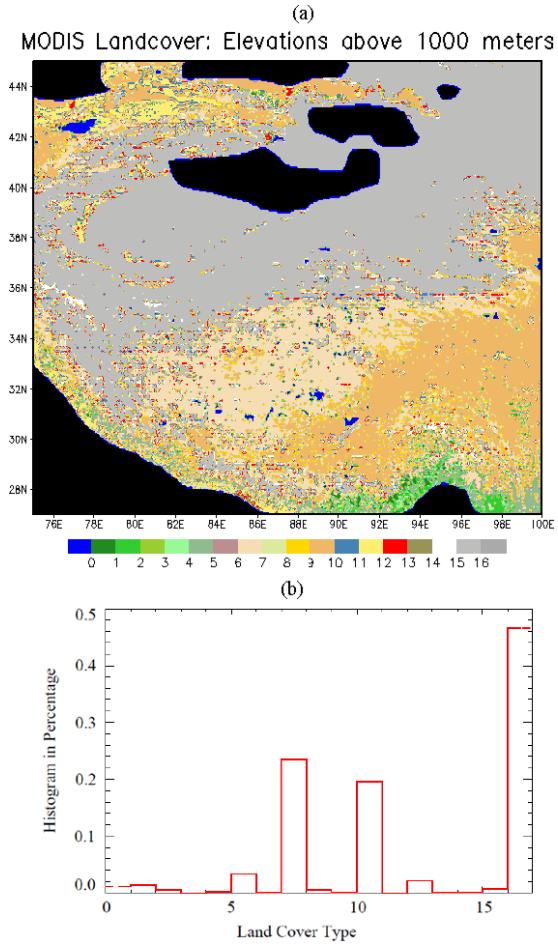

Figure 1. (a) Land cover from MODIS observation at 0.05° × 0.05° resolution for all regions with an elevation higher than 1000 m. Region elevation lower than 1000 m is marked in black color. (b) The percentage of each kind of land cover over the selected analyze region (75–100°E, 27–45°N). Land cover is defines as: 0, water; 1, evergreen needleleaf forest; 2, evergreen broadleaf; 3, deciduous needleleaf forest; 4, deciduous broadleaf forest; 5, mixed forests; 6, closed shrublands; 7, open shrublands; 8, woody savannas; 9, savannas; 10, grasslands; 11, permanent wetlands; 12, croplands; 13, urban and built-up; 14, cropland/natural vegetation mosaic; 15, snow and ice; 16, barren or sparsely vegetated.

3. Results

The spatial land cover map (figure 1(a)) at 0.05° × 0.05° reveals the details of the land type over the Tibetan plateau. Forty-five per cent of the selected study region over the Tibetan plateau (27–45°N, 75–100°E) is barren or sparsely vegetated (namely, land cover type (lc) = 16, figure 1(b)), largely located in the northwest of the Tibetan plateau. Open shrubland is the second most abundant land cover (lc = 7, 20.5%), and grassland is third (lc = 10, 18.6%). Cropland (lc = 12) covers only 6.9% and mixed forest (lc = 5) is only 3.4%, located at south mountains and southwest part of the region.

A warming of the daytime land skin temperature at about 0.4 °C/decade has occurred for the last decade (2000–10) as shown by the positive regression trend detected in the region-averaged skin temperature (figure 2(a)). Because there

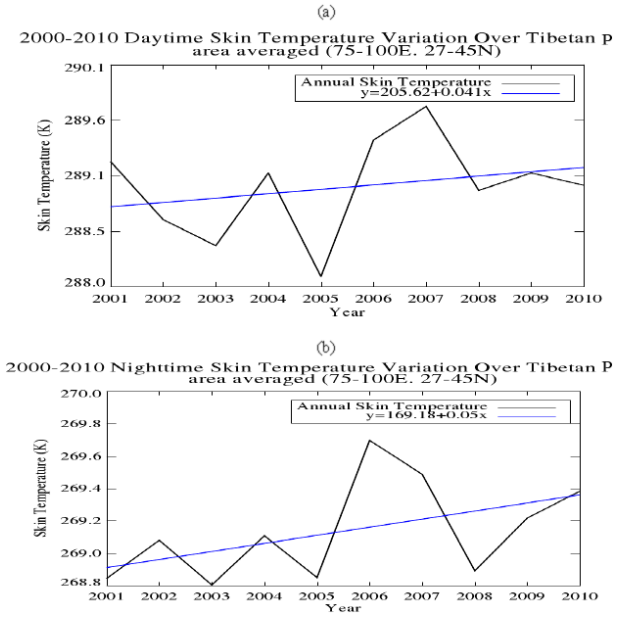

Figure 2. Trend of skin temperature over Tibetan plateau (75–100°E, 27–45°N) for (a) annual daytime based on MODIS Terra (10:30 AM) and (b) annual nighttime based on Terra MODIS (10:30 PM).

is no reason to assume that the temperature variation should follow a normal distribution, a Monte Carlo method (Wilks 1995) rather than a *t*-test is used to examine the trend significance (as applied to skin temperature trend analysis in Jin and Dickinson 2002). According to this test, the warming is statistically significant, but uncertainty remains due to the short duration of observation period. In addition, the annual nighttime skin temperatures also increased at 0.5 °C/decade, which is slightly larger than that of the daytime skin temperature (figure 2(b)). Nevertheless, different land covers have different signals. For example, daytime skin temperatures for barren regions in fact experience a slight cooling trend (figure 3(a)) but a warming at night time (figure 3(b)). This result is consistent with the previous ground-based data analysis reporting that surface air temperature significantly increases at night (Duan and Wu 2006). Duan and Wu (2006) also shows that low-level cloud amounts significantly increase, which may lead to a strong cloud 'greenhouse effect' which warms the surface.

Note that although barren or sparsely vegetated land cover (lc = 16, or bare soil region) is above 40% in our selected region, its increase at night time during 2001–10 (figure 3(b)) is slightly smaller than that of the whole region average (figure 2(b)). In addition, a slight daytime temperature decrease is observed for bare soil, while the whole region is warming at. This may lead to a few possibilities: (a) some other land covers, such as snow-covered region or vegetation region, may experience significant change that overcomes the temperature decrease over the bare soil region; (b) uncertainty of satellite observation needs to be considered in particular when discussing small signal such as temperature trend.

The multi-year averaged diurnal range of skin temperatures between July 2000 and July 2010 over the Tibetan

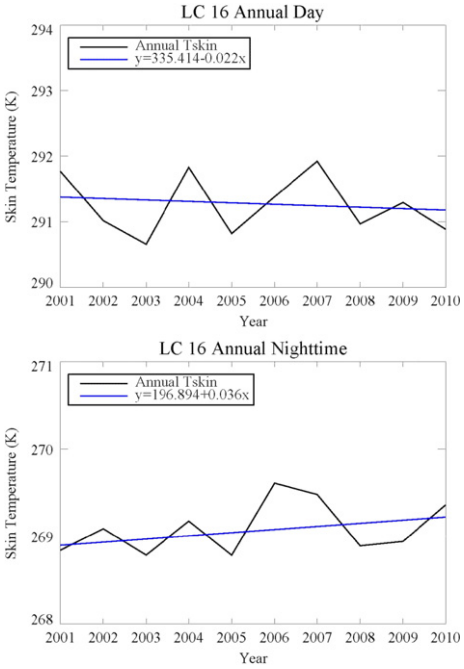

Figure 3. Annual day and night time for barren or sparsely vegetated regions (lc = 16) over Tibetan plateau studied here (70–100°E, 27–45°N).

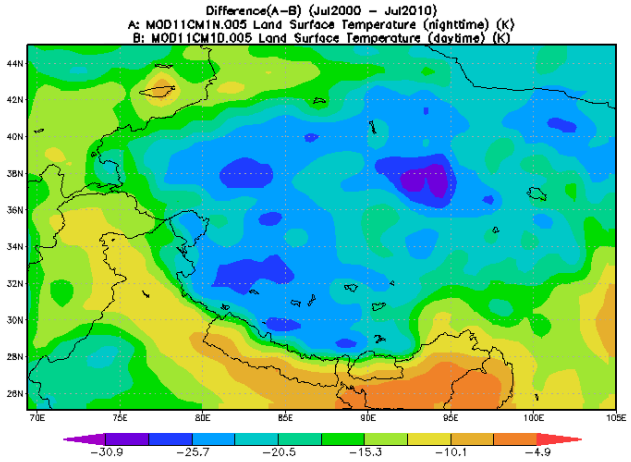

Figure 4. Diurnal range (nighttime minus daytime) of skin temperature averaged from July 2000 to July 2010. Data is from Terra MODIS.

plateau (i.e., nighttime minus daytime, figure 4) shows evident terrain-induced variations. The relatively low-lying arid basins are surrounded by steep elevations that result in elevation differences greater than 3000 m. Areas of elevated terrain, such as the south-facing Himalayan Mountains, experience the least amount of diurnal temperature variation primarily because of the continuous winds, topographical cloud cover and prevention of nocturnal inversion formation (Linacre 1982). In addition, the Tarim Basin in the northwest section of the Tibetan plateau (37–39°N, 81–84°E) and the Qaidam Basin to the east (36–39°N, 90–95°E) have large diurnal ranges (>30 °C).

Table 1. Monthly mean daytime and nighttime land skin temperature for annual, July and January during 2000–10 over Tibetan plateau (75–100°E, 27–45°N). The data is from Terra MODIS at 10:30 AM for daytime and 10:30 PM for nighttime. Note that the earliest observation from Terra is March 2000, so there is no observation for January 2000.

	Annual mean		July		January	
Year	Day	Night	Day	Night	Day	Night
2000			300.1	280.0		
2001	289.2	268.8	301.3	280.2	272.9	256.3
2002	288.6	269.1	299.9	280.2	272.2	256.2
2003	288.4	268.8	298.9	279.5	273.1	257.1
2004	289.1	269.1	300.0	279.6	271.1	256.3
2005	288.1	268.9	299.4	280.2	271.2	256.5
2006	289.4	269.7	301.6	281.1	271.0	257.5
2007	289.7	269.5	300.3	280.1	273.6	256.8
2008	288.9	268.9	300.1	280.1	271.2	254.6
2009	289.1	269.2	300.8	279.8	272.9	257.6
2010	289.0	269.4	300.3	280.9	273.1	257.9

The region-averaged daytime and nighttime skin temperature for the annual means, July and January show clear diurnal, seasonal and inter-annual variations (table 1). For example, in the high elevation plateau, seasonality is evident mainly as a result of solar radiation variation during the year. The warmest year during this period of time is 2007, with an annual mean daytime temperature of 289.7 K and July and January means of 300.3 K and 273.6 K, respectively. The coldest year is 2005, with an annual mean daytime temperature of 288.1 K and means of 299.4 K and 271.1 K for July and January, respectively. Furthermore, the inter-annual variations in January seem to be larger than those in July. In January, the difference between the warmest night (257.9 K in 2010) and the coldest night (254.6 K in 2008) year is 3.3 K, while in July, the difference is only 1.3 K (maximum is 280.9 K in 2010 versus minimum 279.6 K in 2003).

The winter of 2008 has been reported as the coldest winter world-wide of the 21st century, as shown by the globally averaged monthly mean surface air temperature observations (Trenberth 2009). Trenberth (2009), along with various other studies, suggested that a large La Niña event occurred during the winter of 2008 that caused surface rainfall anomalies over the land surface, increasing surface evaporation, and reducing surface temperature. In addition, higher snow cover was observed, resulting in higher surface albedo and less surface insolation. Apparently, the Tibetan plateau participated in this global-scale cold anomaly. Finally, the summer of 2010 was found to have the warmest nights (280.9 K) in these 11 yr. The causes of the temperature changes are a source of ongoing research.

The spatial distribution of skin temperature from July, 2000 to April, 2010 shows a close relation to the underlying land cover (figure 5(a)). For the large desert regions (36–42°N), the 11 yr averaged annual skin temperature can be above 300 K (maximum is above 320 K). Over the open shrublands (centered at 33°N, 87°E), relatively high skin temperatures also occurred (>287 K). In contrast, the mountain regions along 28–30°N, 87–99°E have the lowest skin temperatures, i.e., below 273 K due to snow coverage.

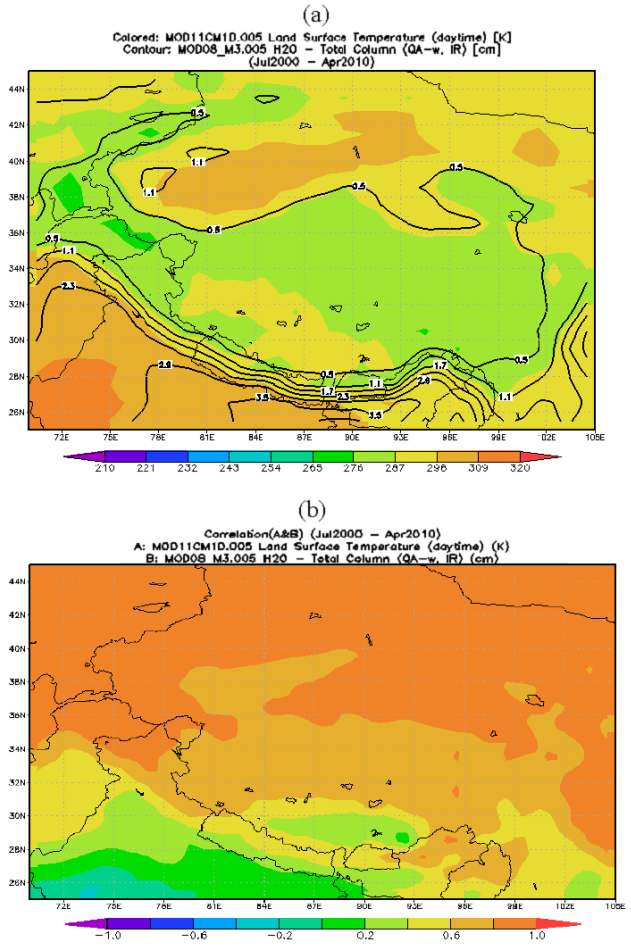

Figure 5. (a) 11 yr (July 2000–April 2010) annual averaged skin temperature and total column water vapor. Skin temperature is in color and water vapor is in contour. (b) Correlation map for 11 yr monthly mean skin temperature and water vapor, data is from July 2000 to April 2010, obtained by Terra MODIS at 10:30 AM. Data resolution is 1° × 1°. Water vapor data is only available until April 2010 when this work is conducted.

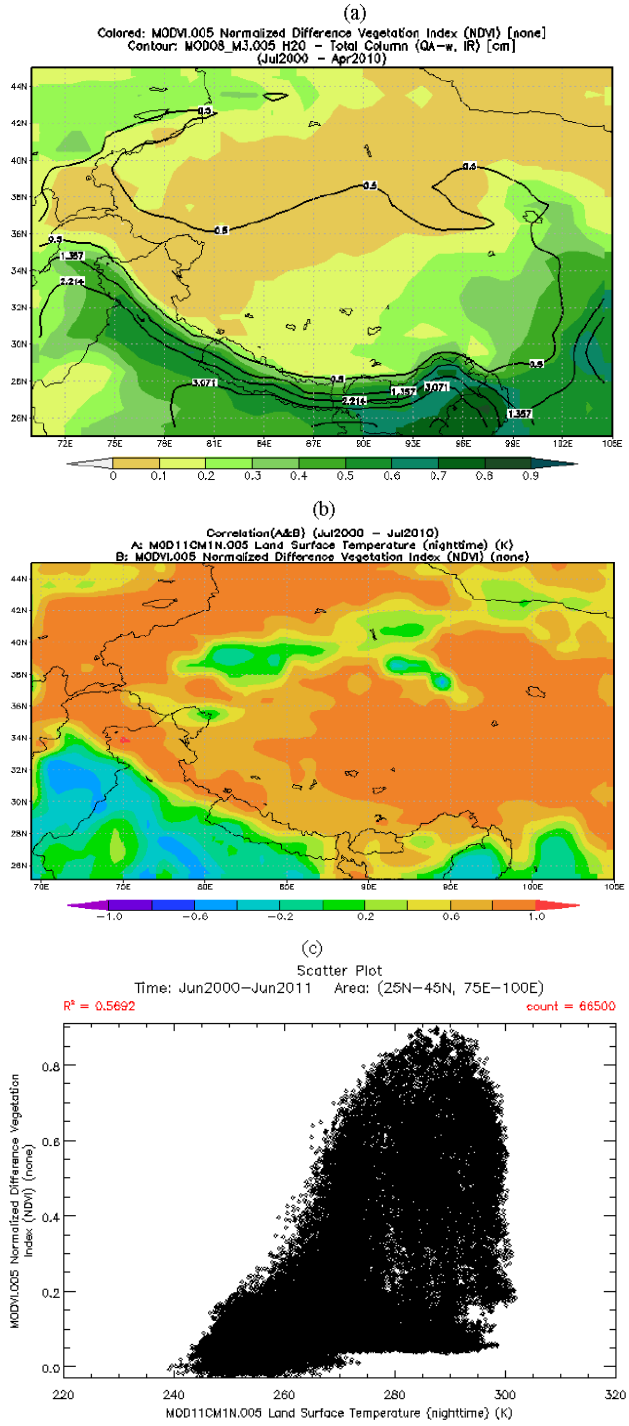

Figure 6. (a) 11 yr (July 2000–April 2010) annual averaged NDVI and total column water vapor. NDVI is in color and water vapor is in contour. Data is from Terra MODIS at 10:30 AM. The available water vapor data is from July 2000–April 2010. Data resolution is 1° × 1°. (b) Correlation map for 11 yr monthly mean skin temperature and NDVI, data is from July 2000 to July 2010, obtained by Terra MODIS at 10:30 AM. Data resolution is 1° × 1°. (c) Scatter plot between monthly skin temperature (x-axis) and monthly NDVI (y-axis). Data is from June 2000 to June 2011, at 1° × 1° resolution from Terra MODIS (10:30 PM).

Skin temperature is in general related to total column water vapor (figure 5(a)) in most regions of Tibetan plateau. The water vapor contours, in particular 0.5 cm contours are closely related to the 276 K skin temperature. However, other factors, such as elevation, monsoon flow, cloud cover rain shadows and vegetation cover all affect water vapor content and skin temperature. For example, areas of higher elevation over the southwest plateau have less water vapor simply because the cooler air holds less water vapor. Furthermore, most regions over the north plateau have a high correlation with skin temperature—correlation values up to 0.8 (figure 5(b)). Additionally, areas in the southern plateau near the Himalayas have the lowest correlations (values close to 0), as well as areas to the southeast, where there is more moisture caused by the southeasterly monsoonal flows.

The spatial distributions of NDVI and total column precipitable water vapor (figure 6(a)) suggest that evapotranspiration from vegetated soil significantly contributes to the total column water vapor. Although large regions over the plateau have limited water vapor due to their cold temperatures and high elevation, maximum water vapor values (values of 1.5 cm and above) are located in the southern area below the Himalayas and southeast of Tibetan plateau,

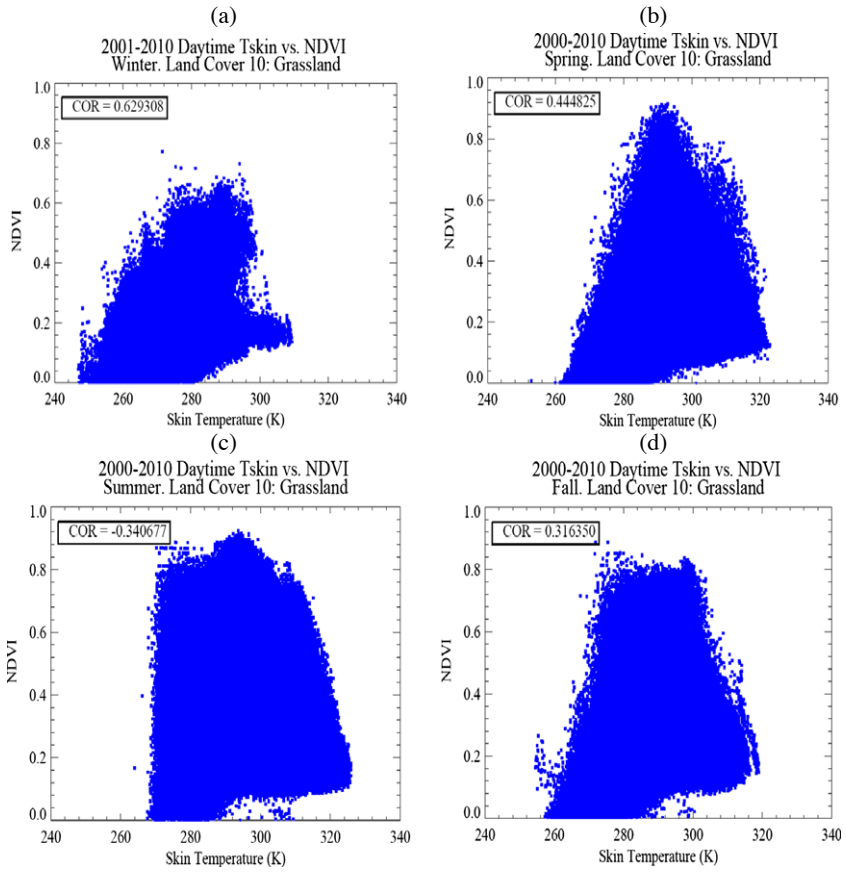

Figure 7. (a) Scatter plot for winter (December, January, February) grassland daytime, monthly mean skin temperature versus NDVI over Tibetan plateau. Data is from Terra MODIS for 2000–10 at 0.05° × 0.05°. (b) Same as (a) except for spring (March, April and May). (c) Same as (a) except for summer (June, July and August). (d) Same as (a) except for fall (September, October and November).

consistent with high NDVI regions (NDVI over 0.9). The areas of lowest water vapor (below 0.5 cm) and NDVI (below 0.1) are located in the northern Tibetan plateau desert regions. Nevertheless, in the southeast plateau (∼98–99°E, 30–34°N), where NDVI values are as high as 0.6, low water vapor values exist there due to the colder air's lower capacity for water vapor. Also, water vapor content changes significantly at the edge of mountains along the southern edge of plateau, mainly due to rain shadow effects and changes in elevation.

Skin temperature and NDVI (figure 6(b)) are highly correlated (coefficients higher than 0.60) over about 90% of the plateau. Low coefficients occur south of the Himalayan Mountains, where southerly monsoonal flow creates a 'rain shadow' resulting in an arid climate with very little rainfall. More interestingly, regions such as the Tarim Basin and Qaidam Basin also have low coefficients (<0.2) because of high temperature, low NDVI and low water vapor. This also demonstrates that the biosphere plays a key role in determining water vapor content via evapotranspiration processes.

A scatter plot of nighttime land skin temperatures and NDVI values from July 2000 to July 2010 shows that high NDVIs (>0.8) occur at high temperatures (>280–295 K), suggesting that vegetation grows in a warm environment better than in a cold environment (figure 6(c)). The NDVI maximum occurs when nighttime temperatures are between 280 and 300 K, and decreases rapidly for temperatures over 300 K, i.e., arid desert regions. Furthermore, at each temperature, NDVI has extreme maximum value. This suggests that a constraint between the skin temperature and vegetation might exist, controlled by land surface energy budget. For example, for temperatures below 280 K, there is a decline in maximum NDVI as the temperature gets colder. Such a relationship has been reported previously (Tucker *et al* 1986) but the reasons are not well understood. In addition, no NDVI values occur for temperature higher than 300 K and no NDVI below 0.05 for temperature above 275 K. Seems that NDVI–skin temperature are constrained in a triangle. Although further research is needed to understand this 'triangle-shape', this shape might be useful to evaluate model simulations. Furthermore, the onset of negative NDVI values, indicating snow and dead organic material, occur at approximately skin temperatures of 273 K and below. Soils and dead organic material typically produce NDVI values of (0.1–0.2) for land skin temperatures above 275 K.

The 'temperature–NDVI triangle-shape' is also evident for individual land cover categories and for daytime observations. For example for grassland land covers, daytime skin temperatures and NDVI show a clear seasonal relation (figure 7). During winter (figure 7(a)), there are two category relations between skin temperature—the first is around 290–300 K with NDVI varying from 0.2 to 0.8. These pixels

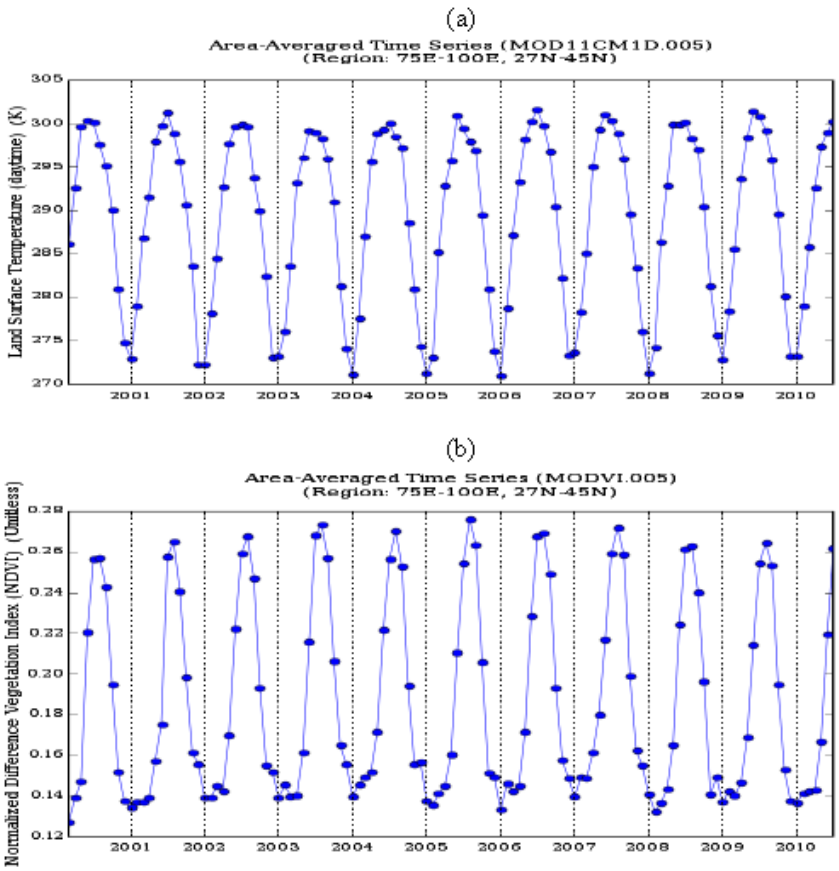

Figure 8. Monthly mean, region-averaged (75–100°E, 27–45°N) (a) land surface skin temperature for daytime from April 2000 to July 2010 and (b) normalized difference vegetation index (NDVI) for the same period of time. Data is from Terra MODIS at observing time of 10:30 AM.

are most likely related to vegetated regions where the surface is hot due to solar radiation. In the second category, skin temperatures are over 295–315 K with NDVI as low as 0.0–0.2, which are likely grassland pixels nearby desert or semi-desert regions. In spring (figure 7(b)), the two categories observed in winter time (figure 7(a)) are merged and a clear 'triangle-shape' appears. This may be due to the growth of vegetation and to the increase of surface insolation in spring. In summer (figure 7(c)) and fall (figure 7(d)), the clear 'triangle-shape' occurs in both seasons. More importantly, for each skin temperature value, there are corresponding NDVI extremes. Such constraints have a similar shape in both spring and fall. This suggests that soil moisture and evaporation may play a role in skin temperature–NDVI extremes, while solar radiation also affects the shapes. Furthermore, the skin temperature–NDVI correlation is as high as 0.63 in winter but only around 0.3–0.4 in spring and fall. In summer, the correlation is negative (−0.34). Again, such 'temperature–NDVI triangle-shape' patterns need further research to be fully understood.

At the monthly, regionally averaged scale, vegetation and skin temperature are closely related to each other, with peak NDVI in mid-summer and low NDVI in winter (figure 8). This correlation is determined by the seasonality of surface insolation as well as the phenology of vegetation. In summer, the availability of ample moisture due to monsoonal precipitations provides a perfect environment for vegetation to grow. The land skin temperature reaches a maximum during the summer season, coinciding with the maximum observed values of NDVI of around 0.34, with most of the plateau being barren and containing little to no vegetation. The regional average includes the lush vegetation-rich areas located on the windward side of the Himalayas, with high values of NDVI that offset the very low values of the rest of the plateau. Although skin temperature and NDVI are related, they are not necessarily linearly related. For example, maximum summer NDVI values in 2003 do not correspond to an abnormally warm skin temperature. Conversely, a maximum summer skin temperature in 2006 did not result at that time an increase of maximum NDVI values.

January 2008 is selected randomly as an example of how winter time snow coverage is for Tibetan plateau region (figure 9). Spatially, the greatest snow amounts occur over high mountain regions in the south edge of the plateau, where the snowmelt in spring and summer feed several important rivers in eastern and southern Asia. Furthermore, high elevation regions over the northern and eastern edges also have abundant snow coverage. Over the region from 27–45°N to 75–100°E about 10% of the area has little or no snow coverage (figure 9(b)), while the rest of the region has snow coverage from 10% to 100%, varying with season.

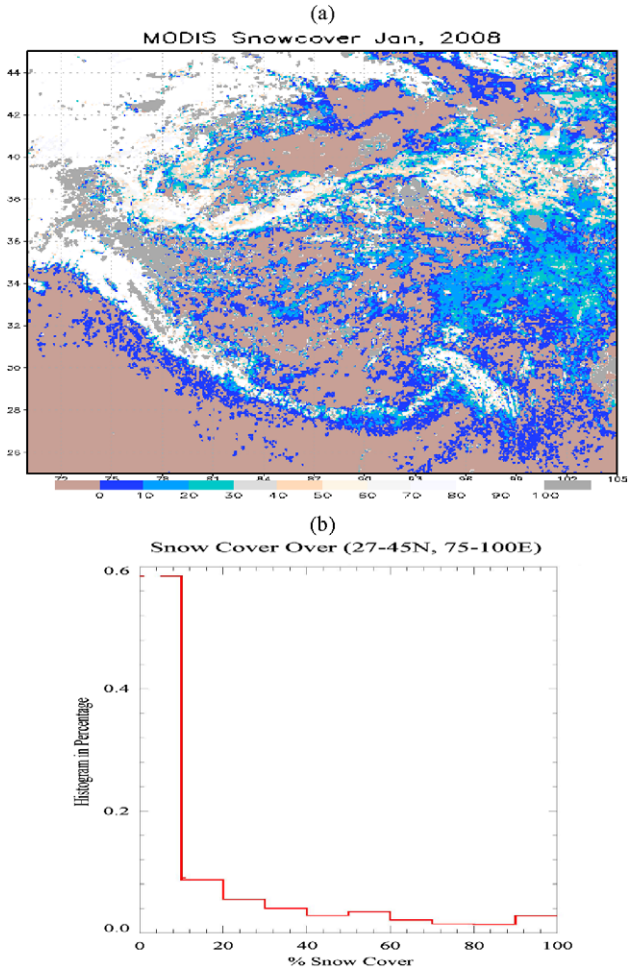

Figure 9. Monthly mean snow coverage for (a) January 2008 from Terra MODIS at the 10:30 AM overpass. (b) Histogram of snow coverage for January 2008, 27–45°N, 75–100°E.

Cloud fraction, as shown in figure 10 for the summer of 2009, clearly affects skin temperatures. Higher cloud fraction reduces surface insolation and thus decreases surface temperature. Since clouds reflect solar radiation but emit longwave radiation at their base temperature, the skin temperature generally follows the cloud fraction pattern. Nevertheless, elevation affects skin temperature since low areas with high cloud cover experience warmer skin temperatures than surrounding higher elevation areas.

4. Final discussion

Since elevation, vegetation and the atmosphere all affect the energy budget of the land surface, land–biosphere–atmosphere interactions determine the diurnal, seasonal and inter-annual variations of skin temperature. On the one hand, vegetation evaporates soil moisture and thus redistributes part of the surface absorbed solar energy to latent heat flux and reduces the Bowen ratio. This mechanism reduces surface temperature. On the other hand, high elevation-induced cold temperatures keep water vapor content low and thus put constraints on vegetation evapotranspiration. Therefore, skin

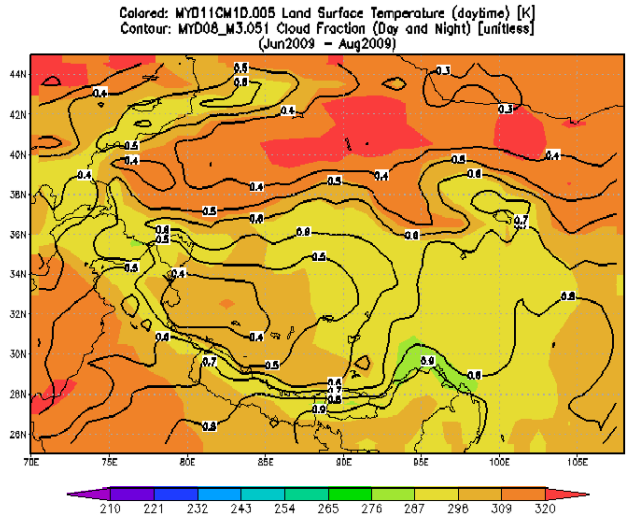

Figure 10. Summer skin temperature and cloud fraction for June, July and August 2009. Skin temperature is in color and cloud fraction is in contour. Data is from Terra MODIS at 10:30 AM at resolution is 1° × 1°.

temperature is determined by the conditions of the biosphere and atmosphere, and in turn plays a critical role in vegetation growth and land-to-atmosphere heat fluxes. Furthermore, the atmosphere, as a response to the large scale dynamics and regional circulation, determines cloud amounts which further affect skin temperature. A significant increase in the amount of low-level clouds over the Tibetan plateau at night has been observed (Duan and Wu 2006), which may lead to skin temperature increases at night time, which is observed in this letter. Aerosols also affect skin temperature, although this is not examined in this work due to the lack of quality observations over such high mountain regions (Jin and Shepherd 2008).

New understandings from this letter include: (a) skin temperature over the whole Tibetan plateau region has a slight warming trend, while the changes may be different for different land covers. Specifically, over the bare soil regions, the trend in skin temperature significantly increases at nighttime, but decreases during the day. (b) Vegetation and skin temperature shows a very clear ‘triangle-shape’ relation. The extreme of the NDVI–skin temperature relation seems to be a function of land cover and seasonality. Further research is needed to better understand this triangle relation. (c) Skin temperature change is closely related to cloud amount and water vapor variations.

The strength of this work is its use of high resolution satellite data. Many results here are consistent with the previous ground-data-based analyses. For example, nighttime skin temperature increasing for bare soil agrees with the increase in low-level cloud amounts reported by Duan and Wu (2006). Our work also leads to a reduced diurnal temperature range (DTR), with the trend in skin temperature decreasing in the daytime and increasing at night. Most importantly, high resolution, independent satellite data provides independent, additional evidence for surface warming over that region. Meanwhile, spontaneous observations for land, biosphere,

cryosphere and atmosphere would be useful to interpret the mechanisms responsible for such a temperature change.

Due to satellite remote sensing uncertainties, these results need to be interpreted with caution. Long-duration observations are needed for surface temperature detection (Jin 2004). Nevertheless, the warming trend presented in figure 1 is based on 10 yr Terra MODIS (10:30 AM, 10:30 PM) measurements, which may not be adequate to establish a trend with confidence. In addition, how these twice-per-day measurements represent the real diurnal cycle of skin temperature over Tibetan plateau needs to be further evaluated with ground measurements, wherever possible.

In conclusion, satellite observations provide high coverage, high resolution observations over the Tibetan plateau. Therefore, these datasets are extremely valuable for examining climate and climate change over the Tibetan plateau and evaluating model simulations for that region.

Further research to understand the existence and cause for the warming detected for this period of time is necessary. Although with its unique elevation and surface conditions, the Tibetan plateau is part of Earth climate system and thus its climate is affected by changes in other regions. For example, changes in SST, as indicated by ENSO, may explain some of the natural variation in the region. Limited by current MODIS data duration, reanalysis or climate modeling may be the only viable approach to address this issue. Nevertheless, a model's capability of simulating the Tibetan land–biosphere–atmosphere interaction should be evaluated before it can be used to study natural variation effects on the Tibetan plateau. The observations reported in this letter may be useful for evaluating model simulations.

Acknowledgments

This work is funded by NSF atmosphere program through grant (ATM0701440) and NASA precipitation program (grant number NNX10 AH65G). Some of the work is analyzed via NASA GIOVANNI online visualization tool.

References

Chu D, Lu L and Zhang T 2007 Sensitivity of normalized difference vegetation index (NDVI) to seasonal and inter-annual climate conditions in Lhasa area, Tibetan plateau *Arct. Antarct. Alp. Res.* **39** 635–41

Duan A M and Wu G X 2006 Change of cloud amount and the climate warming on the Tibetan plateau *Geophys. Res. Lett.* **33** L22704

Gao B-C, Yang P, Guo G, Park S K, Wiscombe W J and Chen B 2003 Measurements of water vapor and high clouds over the Tibetan plateau with the Terra MODIS instrument *IEEE Trans. Geosci. Remote Sens.* **41** 895–900

Hall D K, Riggs G A, Salomonson V V, DiGirolamo N E and Bayr K J 2002 MODIS snow-cover products *Remote. Sens. Environ.* **83** 181–94

Hall D K and Riggs G A 2007 Accuracy assessment of the MODIS snow-cover product *Hydrol. Process.* **21** 1534–47

Jin M 2000 Interpolation of surface radiation temperature measured from polar orbiting satellites to a diurnal cycle. Part 2: cloudy-pixel treatment *J. Geophys. Res.* **105** 4061–76

Jin M 2004 Analyzing skin temperature variations from long-term AVHRR *Bull. Am. Meteorol. Soc.* **85** 587–600

Jin M 2006 MODIS observed seasonal and interannual variations of atmospheric conditions associated with hydrological cycle over Tibetan plateau *Geophys. Res. Lett.* **33** L19707

Jin M and Dickinson R E 2000 A generalized algorithm for retrieving cloudy sky skin temperature from satellite thermal infrared radiances *J. Geophys. Res.* **105** 27037–47

Jin M and Dickinson R E 2002 New observational evidence for global warming from satellite data *Geophys. Res. Lett.* **29** 1400–4

Jin M and Dickinson R E 2010 Land surface skin temperature climatology: benefiting from the strengths of satellite observations *Environ. Res. Lett.* **5** 044004

Jin M and Shepherd J M 2008 Aerosol relationships to warm season clouds and rainfall at monthly scales over east China: urban land versus ocean *J. Geophys. Res.* **113** D24S90

King M D, Menzel W P, Kaufman Y J, Tanré D, Gao B C, Platnick S, Ackerman S A, Remer L A, Pincus R and Hubanks P A 2003 Cloud and aerosol properties, precipitable water, and profiles of temperature and humidity from MODIS *IEEE Trans. Geosci. Remote Sens.* **41** 442–58

Linacre E 1982 The effect of altitude on the daily range of temperature *J. Climatol.* **2** 375–82

Liu X and Chen B 2000 Climatic warming in the Tibetan plateau during recent decades *Int. J. Climatol.* **20** 1729–42

Myneni R B, Hall F G, Sellers P J and Marshak A L 1995 The interpretation of spectral vegetation indexes *IEEE Trans. Geosci. Remote Sens.* **33** 481–6

Trenberth K E 2009 An imperative for climate change planning: tracking earth's global energy *Curr. Opin. Environ. Sustain.* **1** 19–27

Tucker C J, Justice C O and Prince S D 1986 Monitoring the grasslands of the Sahel 1984–1985 *Int. J. Remote Sens.* **7** 1571–81

Wan Z and Li Z-L 2008 Raidance-based validation of the V5 MODIS land-surface temperature product *Int. J. Remote Sens.* **29** 5373–95

Wang B, Bao Q, Hoskins B, Wu G and Liu Y 2008 Tibetan plateau warming and precipitation changes in East Asia *Geophys. Res. Lett.* **35** L14702

Wilks D S 1995 *Statistical Methods in the Atmospheric Sciences—An Introduction* (New York: Academic) p 465

Wu G, Liu Y, Mao J, Liu X and Li W 2004 Adaptation of the atmospheric circulation to thermal forcing over the Tibetan plateau, in observation, theory and modeling of the atmospheric variability *Selected Papers of Nanjing Institute of Meteorology Alumni in Commemoration of Professor Jijia Zhang* ed X Zhu *et al* (Hackensack, NJ: World Scientific) pp 92–114

Wu G and Zhang Y 1998 Tibetan plateau forcing and monsoon onset in south Asia and Southern China sea *Mon. Weather Rev.* **126** 913–27

Yeh T C, Luo S W and Chu P C 1957 The wind structure and heat balance in the lower troposphere over Tibetan plateau and its surroundings *Acta Meteorol. Sin.* **28** 108–21 (in Chinese)